Science in China Series A: Mathematics
2008 Vol. 51 No. 1 1–3
www.scichina.com
www.springerlink.com

A level set method to reconstruct the discontinuity of the conductivity in EIT

Jin Cheng[1] & Wenbin Chen[1]† & Junshan Lin[12] & Lifeng Wang[1]

[1] School of Mathematical Sciences, Fudan University, Shanghai 200433, China;

[2] Department of Mathematics, Michigan State University, East Lansing, MI 48824, USA

Abstract In this paper, one level set method is applied to find the interface of discontinuity of the conductivity in EIT(Electrical impedance tomography) problem. The key of this reconstruction algorithm is to choose the suitable velocity function. The numerical examples demonstrate that the reconstruction algorithm is efficient and stable.

Keywords: EIT, reconstruction algorithm, level set method
MSC(2000): 34K29, 35J05

1 Introduction

Different materials would display different electrical conductivities, thus the conductivity $\sigma(x)$ can be used to infer the internal structure of an object. Due to this fact, Electrical impedance tomography (EIT) has been developed rapidly during the last two decades, and its aim is to recover the interior conductivity from the simultaneous measurements of the voltage and current on the boundary. To describe more rigorously, let $\Omega \subset \mathbb{R}^2$ be a bound object with the conductivity $\sigma(x)$, and suppose that the current flux on the boundary $\partial\Omega$ of a bounded object Ω is $g(x)$, then the electric potential $u(x)$ inside the domain and on the boundary satisfies

$$\nabla \cdot (\sigma \nabla u) = 0 \quad \text{in } \Omega, \qquad \sigma \frac{\partial u}{\partial n} = g \quad \text{on } \partial\Omega, \tag{1}$$

where n denotes the unit outward normal to $\partial\Omega$. Assuming that $\sigma(x) \in L^\infty(\bar{\Omega})$ and $g \in H^{-\frac{1}{2}}(\Omega)$, the above Neumann boundary value problem has a unique solution $u \in H^1(\Omega)$ up to a constant (cf. [16]), where $H^{-\frac{1}{2}}(\Omega)$ and $H^1(\Omega)$ are the standard Sobolev spaces (cf. [1]).

The task of the EIT problem is to determine $\sigma(x)$ from one pair of the boundary voltage and current measurement or several pairs of the boundary voltage and current measurements. Electrical Impedance Tomography is a hopeful imaging tool with important applications. Examples of medical applications of EIT are detection of pulmonary emboli (cf. [8]) and monitoring of heart function (cf. [17]), etc. Besides, there are many important applications in the fields such as geophysics, environmental sciences and nondestructive testing of materials(cf. [26][27][28]).

One of the mathematical formulations of EIT problem was proposed by Caldéron in 1980 (cf. [7]). This problem is called Caldéron problem now, which is to reconstruct the conductivity

Received – –, 2007; accepted – –, 2008
DOI: ————————-

† Corresponding author: Wenbin Chen (email: wbchen@fudan.edu.cn)

This work was partially supported by the Research Foundation for Doctor Programme (Grant No. ———) and the National Natural Science Foundation of China (Grant No. ——)

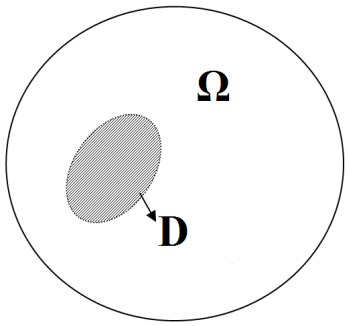

Figure 1: The simplified model with piecewise conductivity σ

from the all boundary voltage and current measurements. The mathematical formulation is to reconstruct the conductivity σ from so called Dirichlet-to-Neumann map $\Lambda_\sigma : H^{\frac{1}{2}}(\Omega) \to H^{-\frac{1}{2}}(\Omega)$. Actually the Caldéron problems inspire the active studies of the inverse problems for partial differential equations.

In this paper, we will assume that $\sigma(x)$ is piecewise constant in Ω, as shown in Figure , i.e.

$$\sigma = \begin{cases} \sigma^+ & x \in \bar{D}, \\ \sigma^- & x \in \bar{\Omega}\backslash\bar{D}. \end{cases}$$

Furthermore, we assume that the conductivity satisfies $\sigma^+ \gg \sigma^-$. This happens in the oil extraction industry where water is injected in a reservoir to force the oil out (cf. [32]), and to estimate the fraction of water is important.

The water typically has a high salt content and is therefore highly conductive. In our formulation, $\bar{D}$ is water surrounded by oil in $\bar{\Omega}\backslash\bar{D}$, and according to the practical experiments, the electric potential in the region of water is close to zero (cf. [32]). Therefore, we are ready to set up one simplified model of original EIT, that is

$$\begin{cases} \Delta u = 0 & \text{in } \Omega\backslash\bar{D}\ , \\ u = 0 & \text{on } \partial D, \\ \dfrac{\partial u}{\partial n} = g & \text{on } \partial\Omega, \\ u = f & \text{on } \partial\Omega, \end{cases} \tag{2}$$

and where the function f is the electric potential measurement on the boundary $\partial\Omega$.

The inverse problem we discuss in this paper is to reconstruct the domain D from one pair (f, g). From the practical point of view, the purpose of this study is to find a effective and fast algorithm to reconstruct the interface surface ∂D. To our knowledge, there are mainly two categories of reconstruction methods for the EIT problem: direct reconstruction algorithms and iterative ones. The direct methods include the so called factorization method proposed by Hank and Brühl (cf. [4],[5], [6]), and reconstruction algorithms based on the formula in the uniqueness proof by Nachmann (cf. [22],[30]). Such direct methods are fast, however, all the information of the DtN mapping Λ_σ is required, which is often impractical. The iterative methods include the

output least squares method (cf. [8]) and the variational method proposed by Kohn (cf. [21]), which are both based on the solutions of the nonlinear optimization problems. However, due to strong non-linearity and severely ill-posedness of the problems, conventional EIT algorithms may only yield poor resolution images.

In this paper, we propose a level set method to reconstruct the interface ∂D. The level set method was proposed by Osher and Sethian in their seminar paper (cf. [25]) to simulate propagating fronts and interfaces. Now it has became a powerful tool to simulate the evolution of interface, this is due to the fact that the level set technique can handle topological changes automatically and effectively. The level set method has been applied successfully in many areas, especially in image processing and computational physics (cf. [24]). However, its applications to inverse problems have just emerged. In 1996, Santosa pointed out how this technique can be applied to the solution of inverse problems involving obstacles (cf. [29]). Since then, the level set methods have been widely used for the inverse problems in partial differential equations. For instance, the level set method has been developed for the inverse scattering problems, here we refer to Dorn and Lesselier's review paper(cf. [15]). Chan and Tai also successfully proposed the level set techniques for a problem similar to (1). However, they are interested to consider the problem where the u or ∇u is essentially available at every point of Ω (cf. [9], [10]). While in our paper, we only assume that the boundary data is known. Now we explain how we can use the level set method to decide the domain D if only the values on the boundary $\partial\Omega$ are measured.

We introduce an auxiliary time variable t, and the domain D is replaced by the domain D_t with the boundary ∂D_t, the potential $u(x)$ is also replaced by $u(t,x)$ correspondingly. At time t, when the boundary ∂D_t is fixed, then $u(t,x)$ satisfies the following boundary value problem:

$$\begin{cases} \Delta u(t,x) = 0 & x \in \Omega \backslash \bar{D}_t \\ u(t,x) = 0 & x \in \partial D_t, \\ \frac{\partial u(t,x)}{\partial n} = g(x) & x \in \partial\Omega. \end{cases} \tag{3}$$

Now we defined the map $F : \mathbb{R}^2 \to L^2(\partial\Omega)$ as follows

$$F(D_t) = u(t,x) \quad x \in \partial\Omega. \tag{4}$$

Comparing it with the original problem (2), then our task becomes whether we can move the boundary ∂D_t such that $F(D_t)$ will tend to f, therefore $u(t,x)$ will arrive at the stationary state $u(x)$. The level set method is one smart strategy to capture the movement of the boundary: Regarding the interface ∂D_t as the zero level set of the function $\phi(t,x)$, once some proper velocity function $\mathbf{V}(t,x)$ could be found for the boundary ∂D_t , then we could solve the corresponding Hamilton-Jacobi equation

$$\frac{\partial \phi(t,x)}{\partial t} + \mathbf{V}(t,\mathbf{x}) \cdot \nabla \phi(t,x) = 0$$

to simulate the evolution of ∂D_t. Obviously, the key of our algorithm is how to decide the velocity function $\mathbf{V}(t,x)$.

In this paper, illumined by the work of the shape optimization, we can explicitly decide the velocity function $\mathbf{V}(t,x)$ such that

$$\frac{d}{dt} \|F(D_t) - f\|^2_{L^2(\partial\Omega)} < 0.$$

Numerical examples demonstrate that our algorithms are efficient. when D is a single connected domain, or is composed of several inclusions far separated, then the boundary ∂D of D is accurately reconstructed. Moreover, the algorithm is very stable against noise, which is not shared by traditional EIT reconstruction algorithms. Therefore, we believe that our method is hopeful in reconstructing the interface of discontinuity in the conductivity.

The rest of the paper is organized as follows. In section 2, we briefly introduce the level set method and propose a way to choose the velocity such that the cost function $\|F(D_t) - f\|_{L^2(\partial\Omega)}$ will decrease with respect to t. The reconstruction algorithm is constructed for approximating the interface ∂D_t. In section 3, some theoretical results are presented and also the analysis for the Tikhonov regularization is obtained. In section 4, we show the performance of our algorithm by several numerical examples. Some concluding remarks are given in section 5.

2 Reconstruction of interface ∂D based on the level set method

2.1 Level set method

In this subsection, the level set method is introduced briefly, more details can be found in the monograph by Osher and Fedkiw (cf. [24]). Suppose that at time t, the boundary ∂D_t of D_t is evolved with the velocity $\mathbf{V}(t,x)$, then the most direct method to simulate and predict the motion of ∂D_t in the future time is to solve the ordinary differential equation

$$\frac{dx}{dt} = \mathbf{V}(t,x) \tag{5}$$

on ∂D_t. This is a Lagrangian formulation of the interface evolution. Then one has to solve Equation (5) numerically, which means that a set of grids must be put on ∂D_t, and the velocity $\mathbf{V}(t,x)$ is discretized on the grids accordingly. If no topological change ever happens to boundary ∂D_t of D_t, then the Lagrangian formulation is enough to simulate the motion. However, if the velocity field $\mathbf{V}(t,x)$ is going to change the topology of the boundary, just like the one presented in Figure 2, this method will no longer be appropriate, since it is hard to characterize the topological change directly.

In order to overcome this difficulty, a level set function $\phi(t,x)$ are proposed for the boundary ∂D_t, i.e.,

$$\phi : (0,\infty) \times \mathbb{R}^2 \to \mathbb{R}^1, \quad \text{such that } \partial D_t = \{(t,x) \mid \phi(t,x) = 0\}. \tag{6}$$

Usually it is assumed that $\phi < 0$ inside ∂D_t, and $\phi > 0$ outside (see Figure 2). Then we would find that, though topological property of ∂D_t changes when the boundary evolves from left to right, we could just lift up the level set function accordingly to capture the motion of the boundary. Thus the topological change could be handled automatically with the level set function ϕ. The level set method is an Eulerian formulation which is proposed by Osher and Sethian in 1988 to simulate propagating fronts (cf. [25]).

It could be easily seen that the level set function ϕ satisfies the partial differential equation

$$\frac{\partial \phi(t,x)}{\partial t} + \mathbf{V}(t,x) \cdot \nabla \phi(t,x) = 0. \tag{7}$$

It is usually called level set equation and is a Hamilton-Jacobi equation. Moreover, if the interface moves under a velocity field in the normal direction $n(t,x)$, i.e, $\mathbf{V}(t,\mathbf{x}) = v(t,x)\mathbf{n}(t,x)$, then the above level set equation could be reformulated as

$$\frac{\partial \phi(t,x)}{\partial t} + v(t,x) \cdot |\nabla \phi(t,x)| = 0, \tag{8}$$

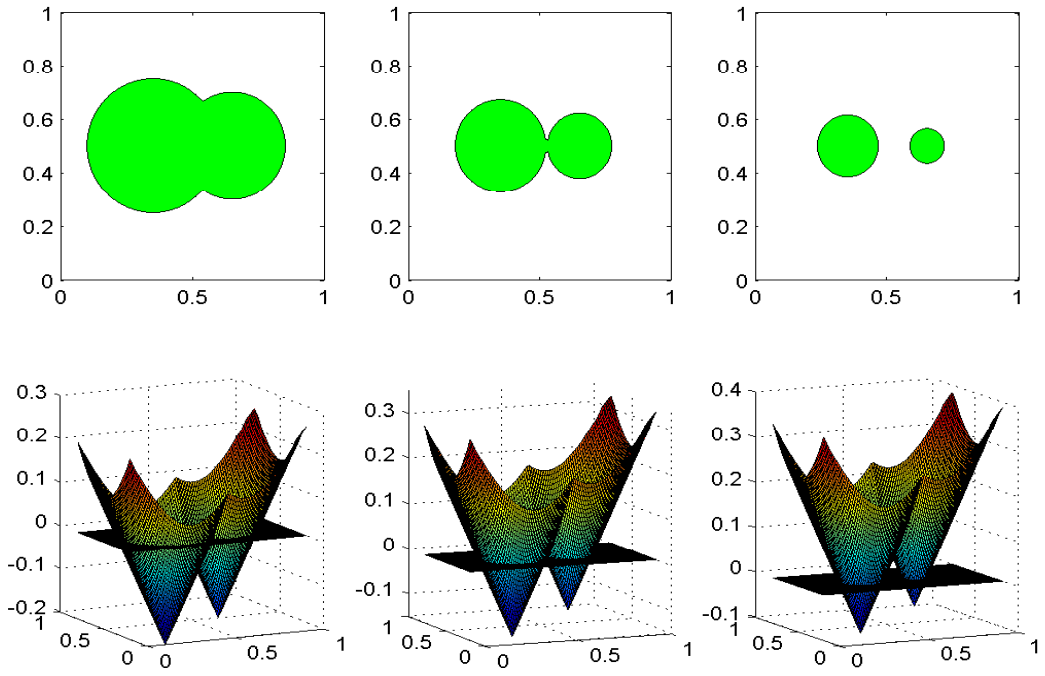

Figure 2: Topological change of the interface(above) and the corresponding level set functions (below).

if we notice that $\mathbf{n}(t,\mathbf{x}) = \dfrac{\nabla\phi(t,x)}{|\nabla\phi(t,x)|}$.

In order to solve (7) and (8) numerically, we could apply the Euler method in the time direction, whereas in the space direction, the simple first-order accurate upwind scheme could be used, or ENO, WENO scheme with higher-order spatial accuracy could be applied (cf. [24]).

2.2 Choice of velocity

In this subsection, we will give the explicit expression of the velocity. Generally, the most direct method to solve (2) is find the solution of the following optimization problem: Find $D \subset \Omega$ such that

$$R(D) = \min_{\tilde{D}\subset\Omega} R(\tilde{D}) \tag{9}$$

and

$$R(\tilde{D}) := \frac{1}{2}\left\|F(\tilde{D}) - f\right\|^2_{L^2(\partial\Omega)} + \alpha\int_{\partial\tilde{D}} 1\, ds, \tag{10}$$

where the map $F : \mathbb{R}^2 \to L^2(\partial\Omega)$ is defined as (4), $\alpha\int_{\partial\tilde{D}} 1\, ds$ is the term of regularization, and $\alpha > 0$ is the regularization parameter, i.e., we would like to penalize the length of the boundary $\partial\tilde{D}$. Such regularization method is often used in image processing (cf. [23]).

In order to explain how we can choose one suitable velocity $\mathbf{V}(t,x)$, let us consider the

problem without regularization, i.e., $\alpha = 0$, then the optimization problem becomes

$$\min_{\tilde{D}\subset\Omega} R_1(\tilde{D}) := \min_{\tilde{D}\subset\Omega} \frac{1}{2} \left\| F(\tilde{D}) - f \right\|^2_{L^2(\partial\Omega)}. \tag{11}$$

Generally, we try to find a 'descent direction', and along the descent direction, $R_1(\tilde{D})$ will be reduced. Equivalently, we would like to find a velocity $\mathbf{V}(t,x)$ for the boundary ∂D_t of D_t such that

$$\frac{d}{dt} R_1(D_t) < 0.$$

For any potential $u(t,x)$ which solves the boundary problem (3), suppose that $u(t+\delta t, x)$ satisfies

$$\begin{cases} \Delta u(t+\delta t, x) = 0 & x \in \Omega \backslash \bar{D}_{t+\delta t}, \\ u(t+\delta t, x) = 0 & x \in \partial D_{t+\delta t}, \\ \dfrac{\partial u(t+\delta t, x)}{\partial n} = g(x) & x \in \partial\Omega. \end{cases}$$

let us define the Eulerian derivative $u'(t,x)$ of $u(t,x)$ as(cf. [15], [31]):

$$u'(t,x) = \lim_{\delta t \to 0+} \frac{u(t+\delta t, x) - u(t,x)}{\delta t},$$

then we have the following lemma.

Lemma 2.1. *The Eulerian derivative $u'(t,x)$ of $u(t,x)$ is the solution of the following boundary problem*

$$\begin{cases} \Delta u'(t,x) = 0 & x \in \Omega \backslash \bar{D}_t, \\ u'(t,x) + \nabla u(t,x) \cdot \mathbf{V}(t,x) = 0 & x \in \partial D_t, \\ \dfrac{\partial u'(t,x)}{\partial n} = 0 & x \in \partial\Omega. \end{cases} \tag{12}$$

This lemma is important for us to choose the velocity $\mathbf{V}(t,x)$, and the proof of the lemma can be found in (cf. [31]).

Theorem 2.1.(Choice of velocity) *Suppose that $D_t \subset \Omega$, $\mathbf{n}(t,x)$ is the unit outward normal to ∂D_t. If the velocity is chosen as $\mathbf{V}(t,x) = v_0(t,x)\mathbf{n}(t,x)$, where the function $v_0(t,x)$ is*

$$v_0(t,x) = \frac{\partial u_1(t,x)}{\partial n} \frac{\partial u_2(t,x)}{\partial n}, \tag{13}$$

and $u_1(t,x)$, $u_2(t,x)$ satisfies the boundary value problems

$$\begin{cases} \Delta u_1(t,x) = 0 & x \in \Omega \backslash \bar{D}_t, \\ u_1(t,x) = 0 & x \in \partial D_t, \\ \dfrac{\partial u_1(t,x)}{\partial n} = g(x) & x \in \partial\Omega, \end{cases} \tag{14}$$

and

$$\begin{cases} \Delta u_2(t,x) = 0 & x \in \Omega \backslash \bar{D}_t, \\ u_2(t,x) = 0 & x \in \partial D_t, \\ \dfrac{\partial u_2(t,x)}{\partial n} = u_1(t,x) - f(x) & x \in \partial\Omega. \end{cases} \tag{15}$$

Then we have

$$\frac{d}{dt}R_1(D_t) < 0.$$

Proof: Let $u'(t,x)$ be the Eulerian derivative of $u_1(t,x)$, and note that on the boundary $\partial\Omega$, the normal derivative of $u_2(t,x)$ is equal to $u_1(t,x) - f(x)$, then it is easy to be checked that

$$\frac{d}{dt}R_1(D_t) = \int_{\partial\Omega}(u_1(t,x) - f(x))u'(t,x)ds = \int_{\partial\Omega}\frac{\partial u_2}{\partial n}u'ds. \tag{16}$$

Note that u_2 and u' both satisfy the Laplace equation (see Equation (15) and Equation (12)), and if we use the the Green's formula: for any $w, v \in H^1(\Omega\backslash D_t)$,

$$\int_{\Omega\backslash D_t}(\Delta wv - \Delta vw)\,dx = \int_{\partial\Omega}\left(\frac{\partial w}{\partial n}v - \frac{\partial v}{\partial n}w\right)ds - \int_{\partial D_t}\left(\frac{\partial w}{\partial n}v - \frac{\partial v}{\partial n}w\right)ds,$$

then

$$\frac{d}{dt}R_1(D_t) = \int_{\partial D_t}\frac{\partial u_2}{\partial n}u'ds.$$

The term of the right hand side can be further transformed if we use the lemma 2.1, that is to say, from the value of Eulerian derivative u' on the interface ∂D_t(see Equation (12)), then

$$\frac{d}{dt}R_1(D_t) = -\int_{\partial D_t}\frac{\partial u_2}{\partial n}(\nabla u_1 \cdot \mathbf{V})\ ds.$$

So if the velocity is chosen as $\mathbf{V}(t,x) = v_0(t,x)\mathbf{n}(t,x)$, and $v_0(t,x)$ is defined as (2.9), then

$$\frac{d}{dt}R_1(D_t) = -\int_{\partial D_t}\left(\frac{\partial u_2}{\partial n}\frac{\partial u_1}{\partial n}\right)^2\ ds < 0.$$

Then we prove the theorem. □

Remark 2.3 Here two comments are given:

1. Note that $u_1|_{\partial D_t} = u_2|_{\partial D_t} = 0$, then the partial derivative of u_1 and u_2 vanish along the tangent direction, therefore, $v_0(t,x)$ can also rewritten as

$$v_0(t,x) = \nabla u_1(t,x) \cdot \nabla u_2(t,x).$$

2. From the proof of this theorem, we know that $\mathbf{V}(t,x)$ is not unique, generally, we can choose

$$\mathbf{V}(t,x) = \omega(t,x)v_0(t,x)\mathbf{n}(t,x),$$

if we require that the weight function $\omega(t,x) > 0$.

For the original problem (9)(10) with the regularization parameter α, we have the following corollary.

Corollary 2.4 *Let $v_0(t,x)$ defined as (2.9) and $\mathbf{n}(t,x)$ be the unit outward normal to D_t. If we set $\mathbf{V}(t,x) = v(t,x)\mathbf{n}(t,x)$ and*

$$v(t,x) = v_0(t,x) - \alpha\kappa(t,x), \tag{17}$$

where κ is the mean curvature of ∂D_t defined by $\kappa = \nabla \cdot \mathbf{n}$, then we have

$$\frac{d}{dt} R(D_t) < 0.$$

Proof: Here the regularization term $\int_{\partial 1 D_t} ds$ is very common, and often used in image processing (cf. [23]) and shape optimization problem (cf. [31]). The Eulerian derivative can be obtained immediately (for example, see (cf. [1])):

$$\frac{d}{dt} \int_{\partial D_t} 1 \, ds = \int_{\partial D_t} \kappa(\mathbf{V} \cdot \mathbf{n}(t,x)) \, ds,$$

Repeating the proof of Theorem 2.1, we can obtain

$$\frac{d}{dt} R(t,x) = - \int_{\partial D_t} (v_0(t,x) - \alpha\kappa)(\mathbf{V} \cdot \mathbf{n}(t,x)) \, ds. \tag{18}$$

Obviously, if we choose $\mathbf{V}(t,x)$ as (2.18), then $\frac{d}{dt} R(t,x) < 0$. □

Therefore, if the velocity on boundary ∂D_t of D_t is defined as in Corollary 2.4, then $\frac{d}{dt} R(D_t) < 0$, i.e., $\mathbf{V}(t,x)$ is a descent direction for $R(D_t)$ at time t. On the other hand, note that $\mathbf{V}(t,x)$ is parallel to the outward unit normal $\mathbf{n}(t,x)$, thus the corresponding level set function $\phi(t,x)$ satisfies

$$\frac{\partial \phi(t,x)}{\partial t} + v(t,x) \, |\nabla \phi(t,x)| = 0.$$

2.3 Reconstruction algorithm

Based on the analysis in the previous subsection, now we are ready to present our reconstruction algorithm. The inputs of the algorithm are the boundary measurements f and g simultaneously, and the output is the interface ∂D_k to approximate ∂D of the EIT problem (2). Our reconstruction algorithm is one standard level set algorithm with the velocity $\mathbf{V}(t,x)$ chosen in Corollary 2.4.

Reconstruction algorithm for EIT:

(1) (*Initialization of D_0*). Set the level set function as ϕ^0 at the initial time $t = 0$, let $\partial D_0 = \{(t,x) \mid \phi_0(t,x) = 0\}$, and $D_0 = \{(t,x) \mid \phi_0(t,x) < 0\}$.

(2) (*Update u_1^k and u_2^k*). For $k = 0, 1, 2, \cdots$, solve the boundary value problems

$$\begin{cases} \Delta u_1^k = 0 & \text{in } \Omega \backslash \bar{D}_k, \\ u_1^k = 0 & \text{on } \partial D_k, \\ \dfrac{\partial u_1^k}{\partial n} = g & \text{on } \partial\Omega, \end{cases} \quad \text{and} \quad \begin{cases} \Delta u_2^k = 0 & \text{on } \Omega \backslash \bar{D}_k, \\ u_2^k = 0 & \text{on } \partial D_k, \\ \dfrac{\partial u_2^k}{\partial n} = u_1^k - f & \text{on } \partial\Omega. \end{cases} \tag{19}$$

If $\left\| u_1^k - f \right\|^2_{L^2(\partial\Omega)} < \epsilon$, where ϵ is a given tolerance, then the iteration is stopped, whereas goes to (3).

(3) (*Choose the velocity*). Suppose that the level set equation is discretized on rectangular grids G in space direction, then we set $v^k = \nabla u_1^k \cdot \nabla u_2^k - \alpha\kappa^k$ on grids which lie in domain $\Omega\backslash\bar{D_k}$. For grids lie in D_k, we interpolate v^k linearly on every row of grids.

(4) (*Update the level set function*). Solve the level set equation $\dfrac{\partial\phi^k}{\partial t} + v^k\left|\nabla\phi^k\right| = 0$. The time direction is discrtized in Euler formula, i.e., $\dfrac{\phi^{k+1}-\phi^k}{\triangle t} + v^k\left|\nabla\phi^k\right| = 0$. In space direction, we use ENO or WENO formula, where the length of time step $\triangle t$ and space time $\triangle x$ satisfy the stability condition of the difference scheme.

(5) (*Reinitialization of* ϕ^{k+1}). Initialize periodically the level set function ϕ^{k+1} to a signed distance function if necessary.

(6) (*Update* D_{k+1}). Find the zero level set ∂D_{k+1} of ϕ^{k+1}, i.e.,

$$\partial D_{k+1} = \{(t,x) \mid \phi^{k+1}(t,\mathbf{x}) = 0\},$$

set $D_{k+1} = \{(t,x) \mid \phi^{k+1}(t,\mathbf{x}) < 0\}$ and goes to (2).

During each iteration, we solve boundary value problems (19) in step (2) and choose the velocity v^k in step (3) to get the velocity of boundary ∂D_k of D_k along the outward normal direction. Just as we have proven in the previous subsection, v^k is a descent direction of $\left\|u_1^k - f\right\|_{L^2(\partial\Omega)}$, i.e $\|F(D_k) - f\|_{L^2(\partial\Omega)}$, where F is defined as (4). On the other hand, we introduce the level set function ϕ^k and solve the Hamilton-Jacobi equaiton $\dfrac{\partial\phi^k}{\partial t} + v^k\left|\nabla\phi^k\right| = 0$ in order to capture the evolution of boundary ∂D_k. Moreover, the criterion for the stop of iteration is to estimate whether $\left\|u_1^k - f\right\|^2_{L^2(\partial\Omega)} < \epsilon$. It should be noted that after solution of the Hamilton-Jacobi numerically in step (3), we would reinitialize the level set function ϕ^{k+1} periodically if necessary. The reason is that only the sign of the level set function ϕ^{k+1}, i.e. the zero level set ∂D_{k+1}, is critical, while the value of ϕ^{k+1} itself is not that important. Thus if ϕ^{k+1} is a singed distance function, then ∂D_{k+1} could be more accurately detected. For more details about the construction of the signed distance function, we refer to the Chapter 7 of [24].

3 Theoretical results for EIT problem and Tikhonov regularization

In this section, we will give some theoretical results for the inverse problem (2) and the Tikhonov regularization. Because of the page limitation of this paper, instead of giving the detail proofs, we only present the results and refer to some related references.

First we discuss the uniqueness and stability of EIT problems.

Assume that the domains $\overline{D}_j \subset \Omega$, $j = 1, 2$, and the boundaries of these two domains can be described by the following parameter equations:

$$\begin{cases} x = \varphi_j(t), \\ y = \psi_j(t), \end{cases}$$

where the parameter $t \in [0, T]$.

Consider the EIT problem:

$$\begin{cases} \Delta u_j = 0 & \text{in } \Omega \backslash \bar{D}_j \ , \\ u_j = 0 & \text{on } \partial D_j, \qquad\qquad j = 1, 2 \\ \dfrac{\partial u_j}{\partial n} = g & \text{on } \partial\Omega, \\ u_j = f_j & \text{on } \partial\Omega, \end{cases} \tag{20}$$

Theorem 3.1. *Suppose that $f_1 = f_2$, on $\partial\Omega$ in the EIT problems* (20) *and $g \neq 0$. We have that*

$$D_1 = D_2.$$

For proving this theorem, we will use the unique continuation for the solutions of Lapalce equations. The reader can refer to the references [2] [3] and [12].

Since the embedding from Sobolev space $W^{1.1}$ to the space of the continuous functions in one dimensional case is compact, by the similar method in [12], we can prove the following conditional stability results for our problem.

Theorem 3.2. *Suppose that $\|g\|_{L^\infty} > c_0 > 0$ and $\|\varphi_j\|_{W^{1,1}} \leq M, \quad \|\psi_j\|_{W^{1,1}} \leq M$ in the EIT problem* (20)*. Here c_0 and M are given constants. Then there are constants $C > 0$ and $0 < \gamma < 1$, which depend on Ω, M and c_0, such that*

$$\operatorname{dist}(D_1, D_2) \leq C \left(\frac{1}{|\log |\log \|f_1 - f_2\|_{L^2}||} \right)^\gamma .$$

Remark 3.3. From the results in Theorem 3.2, we know that the EIT problem we discuss in this paper is a severely ill-posed problem.

As for the Tikhonov functional $R(D)$ we proposed in the previous section, we have the following results:

Theorem 3.4. *For the Tikhonov functional $R(D)$, there exists a $D_* : \varphi_*(t), \psi_*(t) \in W^{1,1}(0, T)$ such that*

$$R(D_*) = \min_{D \in W^{1,1}} R(D)$$

where $D \in W^{1,1}$ means that the parameter representation $\varphi(t), \psi(t) \in W^{1,1}(0, T)$.

This theorem can be proved by the methods which are used in [11] and [18]. We mainly use the fact that the embedding from Sobolev space $W^{1.1}$ to the space of the continuous functions in one dimensional case is compact. We will not give the detail proof here.

Finally, we should point out that, by the results in [13], the conditional stability in Theorem 3.2 implies that convergence rate of the Tikhonov regularized solution.

Theorem 3.5. *Suppose that the EIT problem* (2) *has the exact solution $D : \varphi(t), \psi(t)$ and the data f contains some error, i.e., we know f^δ, which satisfies*

$$\|f - f^\delta\|_{L^2} \leq \delta.$$

If $D_* : \varphi_*(t), \psi_*(t)$ is the minimizer of the following functional

$$R(D) := \frac{1}{2}\|F(D) - f^\delta\|^2_{L^2(\partial\Omega)} + \alpha \int_{\partial D} 1ds.$$

We take $\alpha = \delta^2$. Then we have that

$$\|\varphi - \varphi_*\|, \|\psi - \psi_*\| \leq C_1 \left(\frac{1}{\log|\log\delta|}\right)^\gamma$$

where $C_1 > 0$ and $0 < \gamma < 1$ are constants.

This theorem can be proved by the method in [13] and the results in Theorem 3.2.

4 Numerical examples

We will demonstrate both the advantage and disadvantage of our algorithm by various numerical examples. In order to test the accuracy of the algorithm we consider both the situations where D is simple connected and multi-connected. Finally, we also demonstrate the noise tolerance of the algorithm. For all the examples, we assume that $\Omega = (0,1) \times (0,1)$, and the current $g = 1$ on the boundary $\partial\Omega$. Generally, due to the existence of the domain D, the simulating data f can not obtained exactly. Here f is solved by the standard second order finite element method, and the maximal mesh size is requested to be less than 0.02, the number of the elements and the degree of the freedom are changed according the domain D. As an example, the mesh and the solution of the Example 3.2 are plotted in Figure 3. In all examples, ϵ is set to be 10^{-6}. The choice of the time step Δ is required to satisfy the CFL stability condition, here we set

$$\sup_x |v^k(x)|\Delta t = \alpha\Delta x,$$

the parameter α is chosen between 0.75 and 0.9 to adjust the moving speed of the level set.

Example 3.1 (D is a simple connected domain) In our first example, the real interface of discontinuity ∂D is an ellipse centered in $(0.4, 0.5)$, with long semi-axis 0.2 and short semi-axis 0.1 respectively (see the solid line Figure 4). We assume that the initial guess ∂D_0 is a circle centered in $(0.5, 0.5)$ with radius 0.4 , that is the dotted line in the Figure 4. It could be seen that the numerical solution ∂D_k (dotted line) is very close to the real interface ∂D when $k = 100$, and ∂D_k almost coincidences with ∂D when $k = 200$. Thus, our algorithm is very accurate and efficient when D is a simple connected domain.

Example 3.2 (D contains several simply connected domains) Here we assume the domain D is composed of two single connected areas D^1 and D^2, where D^1 is a circle with radius 0.1, whereas D^2 is an ellipse with long semi-axis 0.1 and short semi-axis 0.05, respectively. The initial guess is the same as the one in Example 3.1. From Figure 5, we find that when $k = 200$, the topology of ∂D_k has greatly changed, and when $k = 500$, the small areas centered in (b) disappeared such that ∂D_k is close to the real solution.

Example 3.3 (D contains several simply connected domains) We can also consider the multi-connected domain D is composed of three components D^1, D^2 and D^3. However, the distance between each component is not as far as one in Example 3.2. The results are plotted in Figure 6, it could be seen from this figure that when $k = 100$, ∂D_k is an envelope of D^1, D^2

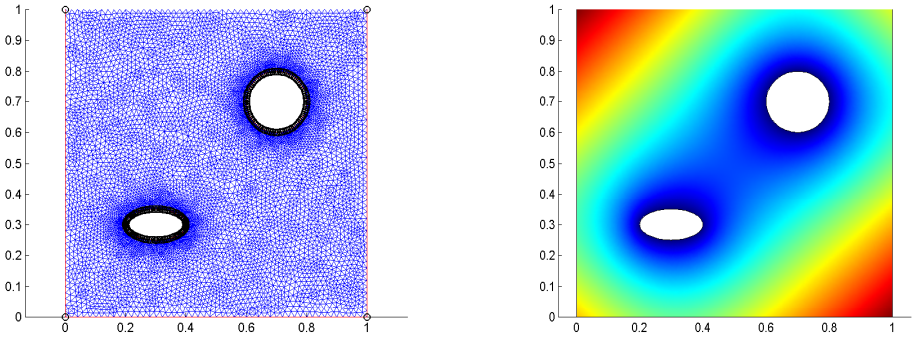

Figure 3: Mesh and finite solution of the forward problem in the Example 3.2, here $g = 1$. Left: the mesh; right: the finite element solution.

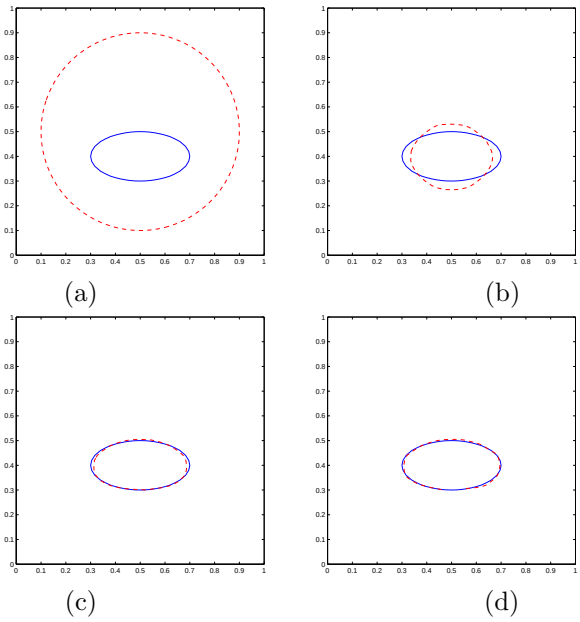

Figure 4: (a)Initial guess; (b) Reconstruction image when $k = 50$; (c) $k = 100$; (d) $k = 200$.

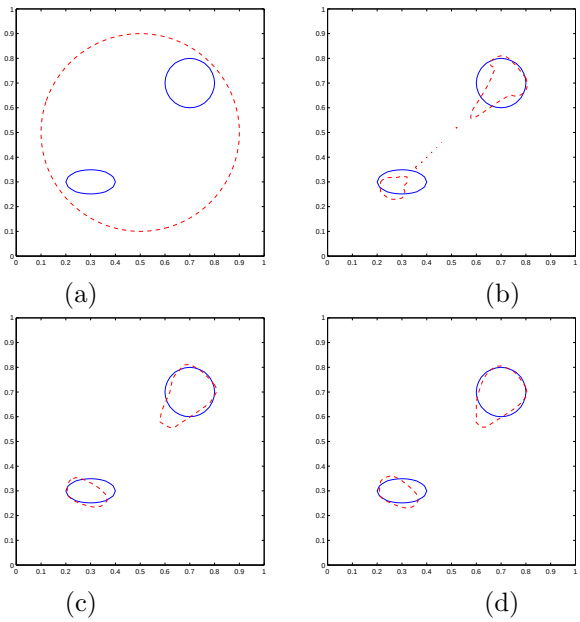

Figure 5: (a)Initial guess; (b) Reconstruction image when $k = 200$; (c) $k = 500$; (d) $k = 1000$.

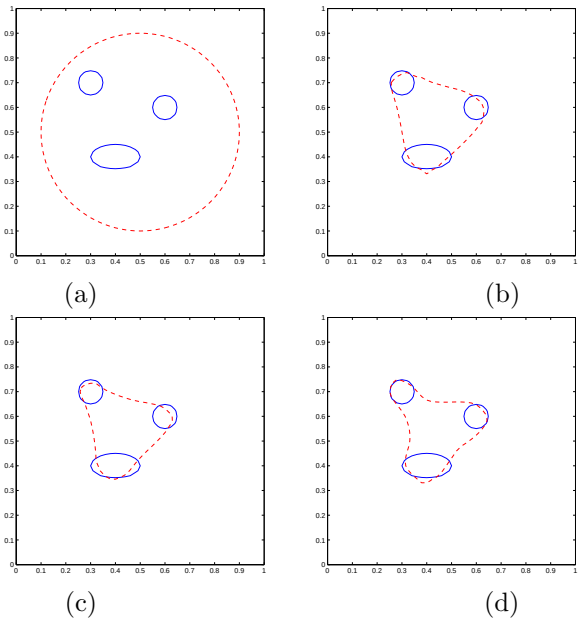

Figure 6: (a)Initial guess; (b) Reconstruction image when $k = 200$; (c) $k = 500$; (d) $k = 1000$.

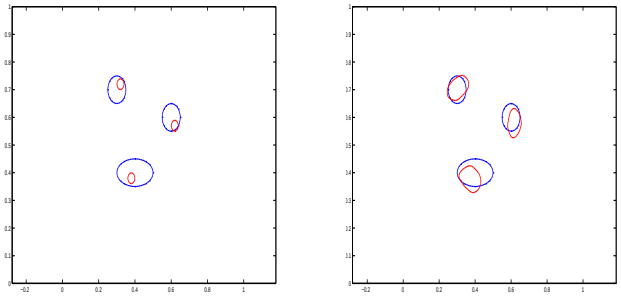

Figure 7: (a) Re-choice of the the initial guess; (b) Reconstruction image when $k = 100$.

and D^3, moreover, the envelope does not make any improvement even when $k = 200$ and 500. We also find that even if more than one current is injected, or the value of current g is changed on the boundary $\partial\Omega$, there is still little improvement of the numerical result. The reason for this phenomenon is that we only get a local minimum solution for the optimization problem (10), rather than the global minimum solution. In the nonlinear optimal problem, obtaining one local minimum instead of the global minimum is a very fundamental problem, which still bothers mathematicians. Thus the resolution of our algorithm is not high enough to identify all the boundaries of components in D when they are near each other.

Example 3.4 (Re-choice of the initial guess) In example 3.3, the contour of level set is an envelop of the unknown domain D, but it is hard to be improved by the iteration. In order to identify all the boundaries of the components in D in Example 3.3, we use one restart strategy to avoid the local minimum point of the optimal problem: Choose three small domains in the envelop as new "seeds", restart the iteration process. Figure 7(a) shows the new initial domains and the 7(b) is the results after 100 iterations, which shows that the domain D can be identified by the new initial guess.

Example 3.5 (Stability) In this example, we will demonstrate the error tolerance of the algorithm. For Example 3.1 and 3.2, when f is solved with the standard second order finite element method, we would add f with an uniformly distributed error with the magnitude of 10%. In our numerical test, we would set the regularization parameter $\alpha = 10^{-3}$, the reconstruction image is plotted in Figure 8(b) and Figure 9(b) respectively. It could be seen that our algorithm is very stable against the noise, this is not shared by common traditional algorithms. On the other hand, we find that the regularization parameter α needs not to be too big, a magnitude of 10^{-3} is totally enough, this also ensure that the time step $\triangle t$ would not be to small when solving the level set equation.

5 Conclusions

In this paper, we apply one level set method for EIT problem and the reconstruction algorithm is proposed. The key of the reconstruction algorithm is to choose suitable velocity function such that the interface ∂D_t will approximate the real interface ∂D. We prove that the cost function $R(D_t)$ can decrease with respect to t if the velocity function $\mathbf{V}(t, x)$ is chosen by our method. The numerical examples show that , when D is a simple connected domain, or is composed of

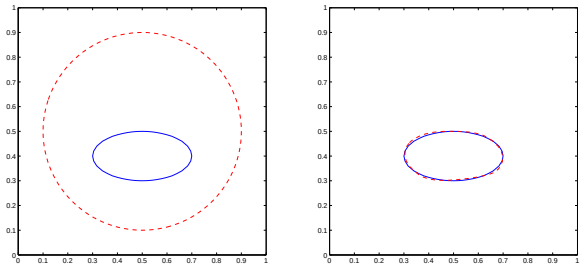

Figure 8: (a)Initial guess; (b) Reconstruction image when $k = 200$.

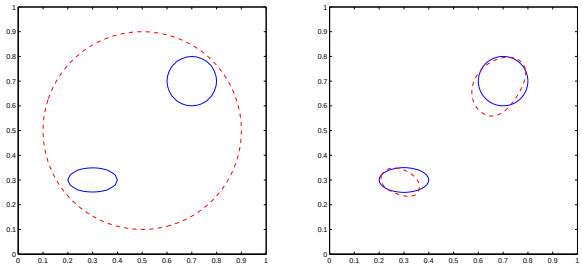

Figure 9: (a)Initial guess; (b) Reconstruction image when $k = 2000$.

several simple connected domains which are not so close to each other, the boundary ∂D of D is accurately reconstructed. For the case that inclusion contains several simple connected domains, which are close to each other, our experiments show that the choice of the initial guess is very important. Actually, we propose one strategy for re-choicing the initial domain.

Compared with the other traditional EIT reconstruction algorithms, our algorithm is very stable against the noise. We believe our reconstruction method is a hopeful method for EIT problem.

Acknowledgements The work is partly supported by NSFC (no. 10431030), the National Basic Research Program under the Grant 2005CB321701 and the 111 project. The authors would like to thank the anonymous referees for their valuable comments.

References

[1] Adams R A, Sobolev Spaces Pure and Applied Mathematics, Vol 65, Academic Press, New York, 1975.

[2] Bukhgeim A L, Cheng J and Yamamoto M, Stability for an inverse boundary problem of determining a part of a boundary. Inverse Problems 15 (1999), no. 4, 1021–1032.

[3] Bukhgeim A L, Cheng J and Yamamoto M, Conditional stability in an inverse problem of determining a non-smooth boundary. J. Math. Anal. Appl. 242 (2000), no. 1, 57–74.

[4] Brühl M and Hank M, Numerical implementation of two noniterative methods for locating inclusions by impedance tomography, *Inverse Problems*, **16**(2000), 1029-1042.

[5] Brühl M and Hank M, Recent progress in electrical impedance tomography, *Inverse Problems*, **19**(2003), 65-90.

[6] Brühl M, Hank M and Pidcock M, Crack detection using electrostatic measurements, *Math. Model. Numer. Anal.*, **35**(2001), 595-605.

[7] Calerón A P, On an inverse boundary problem, *Seminar on Numerical Analysis and its applications to*

Continumm Physics(Soc. Bransileria de Matèmatica, Rio de Janeiro), 1980, 65-73.

[8] Cheney M, Issacson D and Newell J C, Electrical Impedance Tomogrpahy, *SIAM Rev.*, **41**(1999), 85-101.

[9] Chan T F and Tai X-C, Level set and total variation regularization for elliptic inverse problems with discontinuous coefficients, *J. Comput. Phys.*, **193**(2003), 40C66.

[10] Chan T F and Tai X-C, Identification of discontinuous coefficients in elliptic problems using total variation regularisation, *SIAM J. Sci. Comput.*, **25**(2003), 881C904.

[11] Chen Z M and Zou J, An augmented Lagrangian method for identifying discontinuous parameters in elliptic systems. SIAM J. Control Optim. 37 (1999), no. 3, 892–910.

[12] Cheng J, Hon Y C and Yamamoto M, Conditional stability estimation for an inverse boundary problem with non-smooth boundary in $\mathbf{R}^3$. Trans. Amer. Math. Soc. 353 (2001), no. 10, 4123–4138

[13] Cheng J and Yamamoto M, One new strategy for a priori choice of regularizing parameters in Tikhonov's regularization. Inverse Problems 16 (2000), no. 4, L31–L38

[14] Dobson D C, Convergence of a reconstruction method for the inverse conductivity problem, *SIAM J. Appl. Math.*, **8**(1992), 71-81.

[15] Dorn O and Lesselier D, Lever set method for inverse scattering, *Inverse Problems* , **22**(2006), 67-131.

[16] Gilbarg D and Trudinger N S, Elliptic partial differential equations of second order, Springer-Verlag Press, New York, 1983.

[17] Isaacson D and Cheney M, Current Problems in Impedance Imaging, *Inverse Problems in Partial Differential Equantisons*, ed D Colton, R Ewing and W Rundell, SIAM, Philadelphia, PA, 1990, 141-149.

[18] Ito K and Kunisch K, The augmented Lagrangian method for parameter estimation in elliptic systems. SIAM J. Control Optim. 28 (1990), no. 1, 113–136.

[19] Keeller G V, Electrical Property of Rocks and Minerals, Handbook of Physical Constants, ed SPClarck Jr, Geological Society of America, New York, 1988, 553-577.

[20] Kohn R V and Vogelius M, Determining conductivity by boundary measurements, *Commun. Pure Appl. Math.*, **37**(1984), 113C123.

[21] Kohn R V and Vogelius M, Relaxation of a variational method for impedance computed tomography, *Commun. Pure Appl. Math.*, **XL**(1987) 745C777.

[22] Muller J L and Sitanen S, Direct reconstruction of conductivities from boundary measurements, *SIAM J. Sci. Comput.*, **24**(2003), 1232-1266.

[23] Mumford D and Shah J, Optimal approximation by piecewise smooth functions and associated variational problems, *Commun. Pure Appl. Math.*, **42**(1989), 577C685.

[24] Osher S and Fedkiw R, Level set methods and Dynamic Implicit surfaces, Applied Mathematical Sciences, Vol 153, Springer Press, New York, 2003.

[25] Osher S and Sethian JA, Fornts propogating with curvature-dependent speed: algorithms based on Hamilton-Jacobi formulations, *J. Comput. Phys.*, **79**(1988), 12-49.

[26] Parker R L, The inverse problem of resistivity sounding, *Geophysics*, **142**(1984), 2143-2158.

[27] Ramirez A, Daily W, Binley B, LaBreque D and Roelant D, Detection of leaks in underground storage tanks using electrical resistance methods, *J. Environ. Eng. Geophys.*, **1**(1996), 189-203.

[28] Ramirez A, Daily W, LaBreque D, Owen E and Chesnut D, Monitoring an underground steam injection process using electrical resistance tomography, *Water Resources Res.*, **29**(1993), 73-87.

[29] Santosa F, A level set approach for inverse problems involving obstacles, ESAIM, *Control Optim. Calculus Variations* **1**(1996), 17C33.

[30] Siltanen S, Mueller J and Isaacson D, An implementation of the reconstruction algorithm of A. Nachman for 2D inverse conductivity problem, *Inverse Problems*, **16**(2000), 681-699.

[31] Sokolowski J and Zolésio J P, Introduction to Shape Optimization: Shape Sensitivity Analysis, Springer Series in Computational Mathematics, vol 16, Springer Press, Berlin,1992.

[32] Woo H, Kim S, Seo J K, Lionheart W and Woo E J, A direct tracking method for a grounded conductor inside a pipeline from capacitance measurements, *Inverse Problems*,